Cell-derived ECM loaded electrospun nanofibrous scaffolds for periodontal regeneration

Mafalda Santos
mafaldasantos4@tecnico.ulisboa.pt

Instituto Superior Técnico, Lisboa, Portugal

December 2022

Abstract

Periodontitis is an inflammatory infection caused by bacterial plaque accumulation that affects the periodontal tissues supporting the tooth. Current treatments lack bioactive signals to induce tissue repair and coordinated regeneration of the periodontium, thus alternative strategies are needed to improve clinical outcomes. Cell-derived extracellular matrix (ECM) has been used in combination with biomaterials to enhance their biofunctionality for various tissue engineering (TE) applications. In this work, bioactive cell-derived ECM loaded electrospun polycaprolactone/chitosan (PCL/CTS) nanofibrous scaffolds were developed using lyophilized decellularized ECM (dECM) derived from human Periodontal Ligament Stem Cells (PDLSCs). This work's aims were to fabricate and characterize cell-derived ECM electrospun PCL/CTS scaffolds and assess their ability to enhance the osteogenic differentiation of PDLSCs, envisaging periodontal TE applications. Human PDLSCs were cultured and used for dECM production. PDLSCs and dECM were characterized regarding morphology, protein expression, and DNA, glycosaminoglycans and collagen contents. Osteogenic differentiation of PDLSCs was performed on PCL, PCL/CTS and PCL/CTS/ECM electrospun scaffolds for 21 days. The obtained results demonstrate that PCL/CTS/ECM scaffolds promoted cell proliferation compared to PCL and PCL/CTS scaffolds, while maintaining similar physical and mechanical properties of PCL/CTS scaffolds. PCL/CTS/ECM scaffolds enhanced the osteogenic differentiation of PDLSCs, confirmed by increased ALP activity and calcium deposition. PCL/CTS scaffolds showed higher levels of calcium deposition and cell mineralization than PCL scaffolds. Overall, results show that ECM loaded electrospun scaffolds enhanced the osteogenic differentiation and proliferation of PDLSCs. This work describes the first use of lyophilized cell-derived ECM loaded electrospun scaffolds for periodontal TE applications and highlights its potential as a promising therapeutic strategy for periodontitis.

Keywords: Cell-derived Extracellular Matrix; Electrospinning; Periodontal Ligament Stem Cells; Periodontal Regeneration; Tissue Engineering

1. Introduction

Periodontitis is a chronic inflammatory infection of the periodontium, the structure responsible for ensuring tooth attachment and stability. This infection is caused and sustained by bacteria from dental plaque accumulation. In early stages, there is inflammation only of the gingiva, known as gingivitis, which is reversible with effective oral hygiene. However if left untreated, gingivitis progresses to periodontitis. Periodontitis in its advanced form is characterized by the loss and destruction of the periodontium, which is composed of periodontal ligament, root cementum and alveolar bone [1]. The current treatments for periodontitis, such as bone grafts and membranes for guided tissue regeneration, fail to achieve periodontal ligament regeneration and integration of soft and hard tissues [2]. Alternative strategies to treat periodontitis that lead to a coordinated regeneration of all periodontal tissues are needed to improve clinical outcomes.

Tissue engineering (TE) makes use of mediators such as biomaterials, cells, and biochemical factors to facilitate tissue regeneration. Tissue-engineered scaffolds made of synthetic polymers, such as polycaprolactone, polylactic acid and polyethylene glycol, or of natural polymers, such as chitosan, gelatin, alginate, collagen and zein, have been studied for periodontal tissue regeneration [2, 3]. Synthetic polymers offer great mechanical properties suitable for TE strategies, while natural polymers have high biocompatibility. Electrospinning is a versatile technique to produce fibrous scaffolds for various TE approaches. Electrospun nanofibrous membranes can mimic the morphology of extracellular matrix proteins, therefore facilitating cell attachment, proliferation and differentiation. Electrospinning allows the efficient production of micro or nanofibrous scaffolds that

present high porosity, surface area and interconnectivity, which makes these scaffolds highly suitable for the development of periodontal barrier membranes. Polycaprolactone (PCL) is a FDA-approved, biodegradable and biocompatible synthetic material that has been extensively used in biomedical applications. PCL has a slow degradation rate (2-3 years) and good mechanical properties suitable for TE [2]. Chitosan (CTS) is a natural biodegradable material with antibacterial and osteogenic properties. Chitosan is obtained through the deacetylation of chitin, which can be extracted from crustaceans' shells. However, it is highly challenging to electrospin chitosan alone. Moreover, chitosan fibers have poor mechanical properties and rapid degradation [3]. Hence it is usually combined with other polymers, specially synthetic polymers that provide mechanical support. Polycaprolactone and chitosan have already been used together in strategies for periodontal TE. PCL electrospun fibers were coated with drug loaded chitosan nanoparticles to serve as vehicles for the administration of antibiotics [4, 5]. Blends of both polymers were used to produce PCL-CTS blend fibrous scaffolds, that were further complemented with the incorporation of bioactive glass and hydroxyapatite nanoparticles, resulting in enhanced alkaline phosphatase (ALP) activity [6]. Sundaram *et al*. developed a bilayered construct consisted of PCL electrospun fibers to mimic and regenerate PDL, and a CTS scaffold with calcium sulfate to regenerate the alveolar bone [7].

Another key component used in periodontal TE strategies are Periodontal Ligament Stem Cells (PDLSCs). These cells are present in the periodontal ligament (PDL) and serve as a source for progenitor cells, which differentiate into osteoblasts, cementoblasts and fibroblasts, responsible for bone, cementum and PDL formation. These cells can self-renew and differentiate into the osteogenic lineage *in vitro*. PDLSCs have been shown to be able to develop into cementoblast-like cells *in vitro*, and cementum/PDL-like tissue *in vivo*, and to form collagen fibers connecting to the cementum-like tissue, suggesting their potential to regenerate PDL tissue [8].

These cells can be used to produce cell-derived extracellular matrix (ECM) [9]. Decellularized cell-derived ECM (dECM) has been used as scaffolds in several TE strategies, since it closely mimics the *in vivo* microenvironment. ECM influences cell proliferation and differentiation through physical, mechanical and chemical cues [10]. Due to its insufficient mechanical properties, specially when considering hard tissues such as bone, it is often combined with biomaterials, such as electrospun fibers. Thus, dECM can be used in combination with electrospun fibers to further enhance their biofunctionality for various TE applications.

In this work, dECM derived from PDLSCs is combined with electrospun polycaprolactone/chitosan (PCL/CTS) nanofibrous scaffolds to develop bioactive and biomimetic ECM loaded nanofibrous scaffolds with good mechanical properties and antibacterial activity for improved periodontal TE strategies.

2. Methodology

2.1. PDLSC Culture

Human PDLSCs were cultured in low glucose Dulbecco's Modified Eagle's Medium (DMEM, Gibco) supplemented with 10% fetal bovine serum (FBS, Gibco) and 1% antibiotic-antimycotic (A/A, Gibco), at 37℃ and 5% CO_2 in a humidified atmosphere. Medium renewal was performed every 3 to 4 days. To perform cell passaging, PDLSCs were detached using a 0.05% trypsin solution and counted using the Trypan Blue exclusion method.

2.2. dECM Production

PDLSCs were seeded at a density of 3000 cells/cm^2 on 6-well plates with DMEM+10% FBS+ 1% A/A. Cells were expanded for 10 days and medium was renewed every 3 to 4 days. After 10 days, the medium was removed and cells were washed with phosphate buffered saline (PBS, Gibco). The ECM was isolated by a decellularization protocol, using a 0.5% Triton X-100 (Sigma-Aldrich) + 20 mM ammonium hydroxide (NH_4OH, Honeywell) solution in PBS, based on previously reported methods [11, 12]. This solution was added to the wells and incubated for 5min at room temperature. After confirming the occurrence of complete cell lysis and presence of ECM on the wells' surface through microscopic observation, dECM was gently washed 3 times with miliQ water. The dECM was detached using a cell scrapper (Corning) and collected in falcon tubes. The contents of the falcon tubes were lyophilized to obtain dECM in powder form to use in electrospinning.

2.3. Immunocytochemistry Analysis

The presence and distribution of several ECM proteins, namely fibronectin, collagen I, laminin, asporin, osteopontin and osteocalcin, were analyzed in PDLSCs and in decellularized cell-derived ECM, through immunofluorescent stainings.

Cells were seeded on 24-well plates and expanded for 10 days. After the 10 days, cells were washed with PBS and in the case of the ECM the wells of the plates were decellularized and gently washed with miliQ water. The wells with cells or dECM were fixed with 4% paraformaldehyde (PFA) for 20min at room temperature and the immunofluorescent stainings were performed. Wells were

washed with 1% Bovine Serum Albumin (BSA, Sigma-Aldrich) for 5min and then incubated with a blocking solution for 45min, which was composed of 0.3% Triton-X-100, 1% BSA and 10% FBS in PBS. The primary antibodies fibronectin, collagen I, laminin, and asporin were diluted 1:400, osteopontin was diluted 1:200 and osteocalcin 1:50 in blocking solution. The primary antibodies were added and left incubating overnight at 4℃. One well had only one primary antibody from the following: fibronectin (ab6328, Abcam), collagen I (ab34710, Abcam), laminin (ab11575, Abcam), asporin (PA5-28124, Thermo Fisher Scientific), osteopontin (MA5-17180, Thermo Fisher Scientific) and osteocalcin (MAB1419, R&D Systems). After overnight incubation, the primary antibody solution was removed, wells were washed once with 1% BSA, the secondary antibodies diluted 1:500 in 1% BSA were added and left incubating for 1h at room temperature, protected from light. The secondary antibodies were goat anti-rabbit IgG Alexa Fluor 546 (Thermo Fisher Scientific) for wells with collagen I, laminin and asporin; goat anti-mouse IgG Alexa Fluor 546 (Thermo Fisher Scientific) for wells with osteopontin and osteocalcin; and goat anti-mouse IgG Alexa Fluor 488 (Thermo Fisher Scientific) for wells with fibronectin. Finally, secondary antibodies were removed, wells were washed with PBS, the cells' nuclei were counterstained with 1.5 µg/ml DAPI solution (Sigma-Aldrich) for 5min and then washed with PBS. Stainings of the cells/dECM samples were observed by fluorescence microscopy (Leica DMI3000B).

2.4. DNA/GAG/Collagen Quantification

The amount of DNA, glycosaminoglycans (GAGs) and collagen present in samples before and after decellularization was quantified using adequate kits and assays. For samples corresponding to before decellularization, cells were washed with PBS, detached using a 0.05% trypsin solution, centrifuged with miliQ water to form a pellet and the supernatant was removed almost completely. For decellularized samples, the dECM was collected in falcon tubes as described in section 2.2 and lyophilized. In each quantification assay, three samples of each condition (before and after decellularization) were used. DNA present in samples was quantified using Quant-iT PicoGreen dsDNA Reagent and Kit (Thermofisher Scientific) following the manufacturer's instructions. The fluorescence of the samples was measured in triplicates on a plate reader (Infinite 200 Pro; Tecan) at an excitation/emission wavelength of 480/520 nm. DNA concentrations of samples were determined through a standard curve. The amount of GAGs in cells/dECM samples was determined using Dimethyl-Methylene Blue (DMMB) assay. Samples were digested at 60℃ in a 100 µg/ml Papain (P4762, Sigma-Aldrich) solution for 16-18h. A DMMB solution was added to all the samples, and left incubating for 5min at room temperature, protected from light. The absorbance was measured in triplicates on a plate reader (Infinite 200 Pro; Tecan) at 525nm. GAG content of samples was determined through a standard curve. The collagen content of samples was quantified using Hydroxyproline Assay Kit (Sigma-Aldrich) following the manufacturer's instructions. The absorbance of samples was measured in triplicates on a plate reader (Infinite 200 Pro; Tecan) at 560 nm. Collagen content of the different cell/dECM samples was determined through a standard curve.

2.5. Fabrication of Electrospun Scaffolds

Polycaprolactone (PCL, Mn = 70000-90000 Da, Sigma-Aldrich) was dissolved at 13% w/v in 1,1,1,3,3,3-hexafluoro-2-propanol (HFIP, Tokyo Chemical Industry) under agitation for 2.5h at room temperature. Medium molecular weight chitosan (CTS, Mn = 190,000-310,000 Da, Sigma-Aldrich) was dissolved at 5% in a Trifluoroacetic acid (TFA, Honeywell)/Dichloromethane (DCM, Honeywell) (70/30 v/v) solvent mixture and stirred for 1.5h at 250rpm at 50℃, using a magnetic stirrer.

Three solutions were electrospun: PCL solution, PCL-CTS blend solution and PCL-CTS-ECM blend solution. PCL and CTS solutions were blended together to obtain a 70/30 v/v PCL-CTS blend solution, followed by agitation overnight. In the case of PCL-CTS-ECM solution, lyophilized cell-derived ECM was incorporated into the CTS solution (1 mg/ml) and dispersed through agitation for 15min at 300rpm using a magnetic stirrer. Due to CTS presence in the fibers, PCL-CTS and PCL-CTS-ECM scaffolds were crosslinked with glutaraldehyde (GA) vapor (25% v/v, Sigma-Aldrich) for 24h in a desiccator to ensure their stability. Fibrous scaffolds were fabricated using electrospinning. Each solution (5ml) was loaded into a 10ml syringe placed in a pump and connected to a PTFE tube, which was attached to a 21G (inner diameter: 0.8 mm) stainless steel needle. During the electrospinning process for all solutions, a controlled flow rate of 0.5ml/h, an applied voltage of 24kV and a distance of 22cm between needle tip and aluminium foil collector were used. All fibrous scaffolds were electrospun for 2.5h to ensure scaffold thickness, with temperature and relative humidity varying between 23–24℃ and 30–40%, respectively.

2.6. Characterization of Electrospun Scaffolds

2.6.1. Scanning Electron Microscopy

Electrospun fibers were structurally characterized through Scanning Electron Microscopy (SEM) us-

ing a Phenom ProX G6 Desktop SEM (Thermo Fisher Scientific). Samples were coated with a gold/palladium layer and imaged at several magnifications, using an accelerating voltage of 10kV or 15kV. The average fiber diameters of the scaffolds were determined by measuring 100 individual fibers per scaffold from five different SEM images using ImageJ software. The elemental composition of scaffolds was studied through Energy Dispersive X-Ray Analysis (EDX) using the Desktop SEM.

2.6.2. Fourier Transform Infrared Spectroscopy

Attenuated Total Reflectance Fourier Transform Infrared Spectroscopy (ATR-FTIR) analysis was performed using a Bruker AlphaP FTIR spectrometer with Attenuated Total Reflectance platinum–diamond coupling. FTIR spectra were obtained from PCL, PCL-CTS and PCL-CTS-ECM fibrous scaffolds; and from the individual materials, namely PCL, CTS and ECM, in order to confirm their presence in the electrospun scaffolds. Transmittance spectra were obtained with a spectral resolution of 4 cm^{-1} and in the range 4000 to 400 cm^{-1}.

2.6.3. Thermal Properties Analysis

Differential Scanning Calorimetry (DSC) Analysis was performed on a Simultaneous Thermal Analyzer, STA 6000 system (Perkin Elmer). Samples of PCL, PCL-CTS and PCL-CTS-ECM fibers and of the used polymers (PCL and CTS) were weighed in alumina pans and heated from 20 ℃ to 200 ℃ at a heating rate of 10 ℃/min. The thermal degradation of the polymers and the fibers was evaluated using Thermogravimetric Analysis (TGA) mode on the STA 6000 system. The samples were heated from 50 ℃ to 600 ℃ at a heating rate of 10 ℃/min. DSC and TGA were performed in triplicates under a nitrogen atmosphere with a flowrate of 20 ml/min.

2.6.4. Contact Angle

The contact angles of PCL, PCL-CTS and PCL-CTS-ECM fibers were measured using a DSA25 Drop Shape Analyzer (Krüss) in the sessile drop method. Droplets of distilled water were placed on the scaffolds' surface and the contact angles were measured. For each condition, the contact angles were measured in 3 individual fiber samples (N=3).

2.6.5. Mechanical Tensile Testing

The mechanical properties of electrospun scaffolds were assessed through uniaxial tensile testing at room temperature using a mechanical tester (Univert Model UV-200-01, CellScale Biomaterials Testing), with a 10N load cell and a 3mm/min displacement rate. For each condition, ten different test specimens (N=10) were cut as rectangular strips with a length of 30mm, width of 10mm and thickness of 0.1mm. The experimental data was collected and processed using the UniVert software, and was analyzed using Microsoft Excel. The Young's modulus of each specimen was obtained from the slope of the initial linear portion (0-15%) of the stress-strain curve. The ultimate tensile strength (UTS) and ultimate elongation were also obtained from the stress-strain curves.

2.7. In Vitro Cell Culture on Electrospun Scaffolds and Assessment of their Biological Effects

2.7.1. Scaffold preparation and cell seeding

PCL, PCL-CTS and PCL-CTS-ECM electrospun scaffolds were sterilized with UV light for 30min and washed three times with a 1% (v/v) A/A PBS solution. The scaffolds were placed in ultra-low attachment 24-well plates (Corning), washed again with PBS + 1% A/A, then immersed in DMEM+10% FBS+1% A/A and incubated for 1h at 37 ℃. The medium was removed, PDLSCs were seeded at a density of 50.000 cells per scaffold and incubated without culture media for 3h at 37 ℃ and 5% CO_2 to promote initial cell attachment. Osteogenic medium, composed of DMEM supplemented with 10% FBS, 1% A/A, 10 mM β-glycerophosphate (Sigma-Aldrich), 50 µg/ml ascorbic acid (Sigma-Aldrich) and 10 nM dexamethasone (Sigma-Aldrich), was added to all scaffolds. PDLSCs were cultured on the scaffolds for 21 days and medium was renewed every 3-4 days.

2.7.2. PDLSC Proliferation Assay

PDLSC proliferation on electrospun scaffolds was evaluated using AlamarBlue Cell Viability Assay (Thermo Fisher Scientific) on days 1, 7, 14 and 21. A 10% (v/v) AlamarBlue solution in culture medium was added to the scaffolds and incubated at 37 ℃ and 5% CO_2 for 3h. The fluorescence was then measured on a plate reader (Infinite 200 Pro; Tecan) at an excitation/emission wavelength of 560/590 nm and compared to a calibration curve to assess the number of cells in each scaffold. For each condition, the fluorescence was measured for six independent scaffolds (N=6) in triplicates and acellular scaffolds were used as blank controls.

2.7.3. Cell Morphology

To assess the morphology of PDLSCs present on the electrospun scaffolds, DAPI-Phalloidin staining was performed. Cells were washed with PBS, fixed with 4% PFA for 20min and permeabilized with a 0.1% Triton X-100 solution for 10min. Phalloidin (Thermo Fisher Scientific) was diluted 1:100 in PBS, added to the cells and left incubating for 45min at room temperature, protected from light. Then, cells were washed with PBS, counterstained with 1.5 µg/ml DAPI solution for 5min and washed with PBS. The fluorescent stainings were observed by fluorescence microscopy (Leica DMI3000B).

2.7.4. Immunocytochemistry Analysis

The presence of collagen I (Col I), asporin (ASP), osteopontin (OPN), osteocalcin (OC), periostin (POSTN) and cementum protein (CMP) was analyzed in PDLSCs cultured on electrospun scaffolds after 21 days of osteogenic differentiation. The scaffolds were washed once with PBS, fixed with 4% PFA for 20min at room temperature and immunofluorescent stainings were performed. Cells were permeabilized with 1% BSA for 5min and then with a blocking solution for 45min, which was composed of 0.3% Triton-X-100 (Sigma-Aldrich), 1% BSA and 10% FBS in PBS. The primary antibodies asporin, osteopontin, periostin and cementum protein were diluted 1:100, collagen I was diluted 1:200 and osteocalcin 1:50 in the blocking solution. The primary antibodies were added and left incubating overnight at 4℃. One scaffold had only one primary antibody from the following: collagen I (ab34710, Abcam), asporin (PA5-28124, Thermo Fisher Scientific), osteopontin (MA5-17180, Thermo Fisher Scientific), osteocalcin (MAB1419, R&D Systems), periostin (ab14041, Abcam) and cementum protein 1 (PA5-63462, Thermo Fisher Scientific). After overnight incubation, the primary antibody solution was removed, cells were washed once with 1% BSA, the secondary antibodies diluted 1:200 in 1% BSA were added and left incubating for 1h at room temperature, protected from light. The secondary antibodies were goat anti-rabbit IgG Alexa Fluor 546 (Thermo Fisher Scientific) for scaffolds with collagen I, asporin, periostin and cementum protein, and goat anti-mouse IgG Alexa Fluor 546 (Thermo Fisher Scientific) for scaffolds with osteopontin and osteocalcin. Finally, secondary antibodies were removed, cells were washed with PBS, the cells' nuclei were counterstained with 1.5 µg/ml DAPI solution (Sigma-Aldrich) for 5min and then washed with PBS. The immunofluorescent stainings were observed by fluorescence microscopy.

2.7.5. ALP Activity Assay

ALP activity was quantified using QuantiChrom ALP Assay Kit (BioAssays Systems) after 21 days of osteogenic differentiation of PDLSCs cultured on scaffolds. The scaffolds were washed with PBS and incubated with a 0,1% Triton X-100 solution overnight at room temperature under orbital agitation. Then, a 10mM p-nitrophenyl phosphate solution, provided with the kit, was added to the samples. The absorbance was then measured on a plate reader (Infinite 200 Pro; Tecan) at 405nm and normalized to the number of PDLSCs present on each scaffold. For each condition, the absorbance was measured for three independent scaffolds (N=3) in triplicates.

2.7.6. Biomineralization Staining

PDLSCs mineralization on the scaffolds after 21 days of osteogenic differentiation was assessed using OsteoImage Mineralization Assay (Lonza). This assay's staining reagent binds specifically to the hydroxyapatite portion of bone-like nodules deposited by cells. For each experimental group, three scaffolds (N=3) were washed once with PBS, fixed with 4% PFA for 20min at room temperature and washed once with 1X Wash Buffer. Then, diluted staining reagent was added to the scaffolds and left incubating for 30min at room temperature, protected from light. Scaffolds were then washed 3 times with 1X Wash Buffer, the fluorescence was measured on a plate reader (Infinite 200 Pro; Tecan) at an excitation/emission wavelength of 492/520 nm, and the fluorescent staining of the cells was observed by fluorescence microscopy.

2.7.7. Alizarin Red Staining and Quantification

After 21 days of culture, calcium deposition was assessed and quantified with Alizarin Red staining. For each condition, three scaffolds (N=3) were washed once with PBS, fixed with 4% PFA for 20min at room temperature and incubated with a 2% Alizarin Red solution (Sigma-Aldrich) for 1 h at room temperature, protected from light. Then, scaffolds were washed 4 times with miliQ water and imaged under the microscope. Afterwards, the water was removed and the Alizarin Red bound to the scaffolds was dissolved with a 10% (w/v) cetylpyridinium chloride solution under orbital agitation for 1h. The absorbance was measured in triplicates on a plate reader (Infinite 200 Pro; Tecan) at 550nm and compared to a standard curve to determine Alizarin Red concentration.

2.7.8. RNA Extraction and qRT-PCR Analysis

Total RNA was extracted using the RNeasy Mini Kit (QIAGEN) following the manufacturer's instructions. cDNA was synthesized from the purified RNA using High-Capacity cDNA Reverse Transcription kit (Thermofisher Scientific). Reaction mixtures were incubated in a thermal cycler (Biorad) for 5 min at 25℃, 20 min at 46℃ and 1 min at 95℃ and then were maintained at 4℃. The qRT-PCR was performed using NZYSpeedy qPCR Green Master Mix (2x), ROX plus (NZYTech) and StepOnePlus real-time PCR system (Applied Biosystems). Target genes were ALP, Runt-related transcription factor 2 (RUNX2), Col I, OC, CMP and Osterix (OSX). All samples were analyzed in triplicates. Target gene expression was primarily normalized to glyceraldehyde 3-phosphate dehydrogenase (GAPDH) gene expression and then determined as a fold change relative to the baseline target gene's expression in undifferentiated PDLSCs at day 0, prior to scaffold seeding (Control).

2.8. Statistical Analysis

The statistical analysis of the data was performed in GraphPad Prism 9 software using one-way ANOVA, followed by Tukey post-hoc test. Data was considered to be statistically significant when the p-values obtained were less than 0.05 (95% confidence intervals, *p $<$ 0.05).

3. Results & discussion

3.1. Immunocytochemistry Analysis

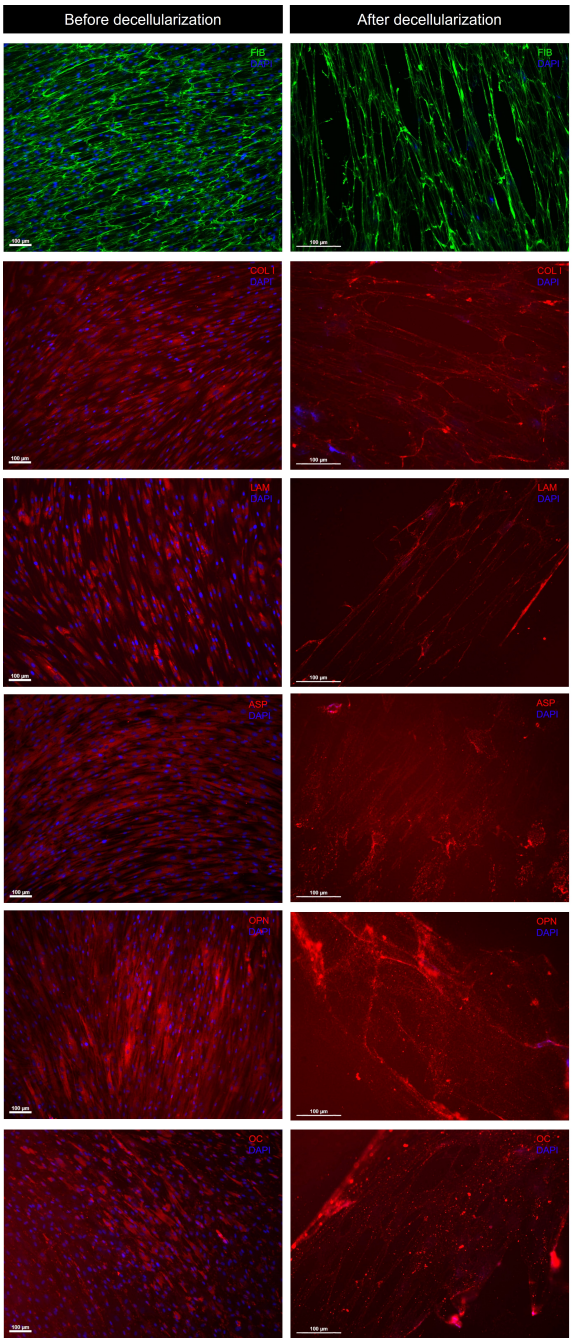

Figure 1: Characterization of PDLSCs and dECM by immunocytochemistry analysis. Immunofluorescent staining images before and after decellularization of: fibronectin (FIB, green), collagen I (COL I, red), laminin (LAM, red), asporin (ASP, red), osteopontin (OPN, red) and osteocalcin (OC, red). Nuclei stained with DAPI (blue). Scale bars 100 µm.

Immunofluorescent staining images (Figure 1) confirm that PDLSCs express all the analysed proteins before decellularization. The expression of these proteins was maintained in decellularized ECM. Collagen I, fibronectin and laminin are three main ECM proteins. It can be observed that decellularized ECM possesses a fibrillary structure composed of these three main ECM proteins, as described in the literature [11, 12]. PDLSCs present a fibroblast-like morphology, clearly visible through collagen I and laminin stainings (Figure 1). Asporin is a protein associated with the periodontal ligament. Osteopontin is a bone ECM protein important for osteogenesis. Osteopontin and osteocalcin are osteogenic markers and are expressed in the periodontium, their positive expression demonstrates that PDLSCs present intrinsic osteogenic potential. After decellularization, only the ECM secreted by the cells remained, thus no cell nuclei are visible with DAPI, confirming successful decellularization.

3.2. DNA/GAG/Collagen Quantification

After decellularization, cell-derived ECM retained to some extent the GAG and collagen content present before decellularization (Figure 2), similar to what is reported in the literature [11, 13]. On the other hand, DNA content is almost completely diminished, confirming successful decellularization.

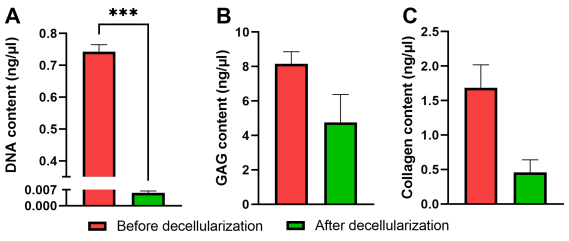

Figure 2: Quantified contents of DNA (A), GAGs (B) and collagen (C). Each quantification was performed on three different samples (N=3) for both conditions; *** p $<$ 0.001.

3.3. Characterization of Electrospun Scaffolds

3.3.1. Scanning Electron Microscopy

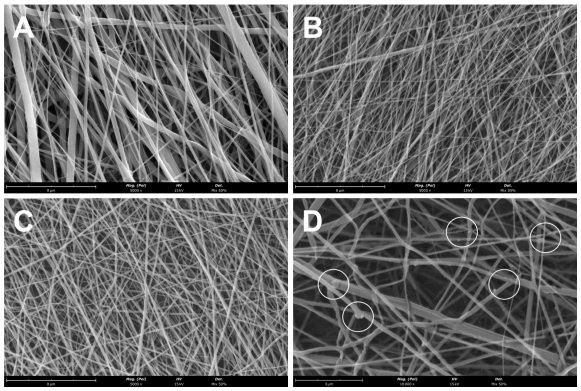

Figure 3: SEM images of PCL (A), PCL-CTS (B) and PCL-CTS-ECM (C) electrospun fibrous scaffolds. Scale bar 8 µm. D) SEM image of dECM particles, identified with white circles, on PCL-CTS-ECM fibers. Scale bar 3 µm.

SEM micrographs (Figure 3) showed that PCL-CTS and PCL-CTS-ECM electrospun scaffolds were composed of beadless and homogeneous nanofibers. However, PCL electrospun scaffolds were more heterogenous, but were still mainly constituted of beadless fibers in the nanometer range. All scaffolds were highly porous and showed high interconnectivity. In PCL-CTS-ECM scaffolds, ECM particles were clearly detected on top of the fibers, as illustrated in Figure 3.

The average fiber diameter of electrospun PCL fibers was 284 $\pm$ 150 nm, whilst the average fiber diameters of PCL-CTS and PCL-CTS-ECM fibers were 121 $\pm$ 27 nm and 127 $\pm$ 25 nm, respectively. The presence of CTS in the fibers led to a significant decrease in the fiber diameter, which is accordance with previous studies [14–16]. PCL-CTS and PCL-CTS-ECM fibers presented similar diameters at the nanoscale, which indicates that the incorporation of decellularized cell-derived ECM did not influence the electrospinning process or alter the average fiber diameter of scaffolds [17]. In table 1, EDX analysis shows that carbon and oxygen were the main constituents of the scaffolds. PCL-CTS and PCL-CTS-ECM scaffolds have similar carbon and oxygen percentages, differing slightly from the PCL scaffolds. Atomic percentages of nitrogen confirm the presence of CTS in the scaffolds. Interestingly, this percentage was slightly higher in PCL-CTS-ECM scaffolds, compared to PCL-CTS scaffolds, which can be due to the presence of ECM that is composed of proteins, a known source of nitrogen.

Table 1: Atomic percentage of carbon, oxygen and nitrogen of PCL, PCL-CTS and PCL-CTS-ECM electrospun scaffolds.

Scaffold	C(%)	O(%)	N(%)
PCL	57.167	27.298	-
PCL-CTS	39.395	38.005	1.829
PCL-CTS-ECM	43.869	36.701	2.794

3.3.2. Fourier Transform Infrared Spectroscopy

The spectra of PCL, PCL-CTS and PCL-CTS-ECM electrospun scaffolds showed all the major characteristic peaks of PCL which confirm PCL presence in the scaffolds: peaks at 2940 and 2865 cm^{-1} corresponding to asymmetric and symmetric C-H_2 stretching, respectively, a pronounced peak at 1725 cm^{-1} that corresponds to ester carbonyl bond stretching; and peaks at 1240 and 1175 cm^{-1} that correspond to asymmetric and symmetric C–O–C stretching, respectively [14–16, 18, 19]. The FTIR spectra of CTS and of ECM show a broad band between 3500 and 3100 cm^{-1} associated with O-H and N-H stretching and a peak at 1640 cm^{-1} related to C=O stretching of amide I. The broad band resulted in a deformation in that region in comparison to the PCL scaffold's spectrum. The peak at 1640 cm^{-1} resulted in a clear deformation around 1670 cm^{-1}, confirming the presence of chitosan in the scaffolds, in agreement with the existing literature [14, 16, 19–21]. Since the ECM and CTS present the same peak and band, it was not possible to see differences in the spectra resulting from ECM incorporation. It is also important to note that a low amount of ECM was present in the PCL-CTS-ECM scaffolds compared to the large amounts of PCL and CTS.

3.3.3. Thermal Properties Analysis

DSC and TGA thermograms, as well as the plots from the first derivative of the mass loss curves (DTGA) of the electrospun scaffolds and the pristine polymers are shown in Figure 4 and their thermal properties in Table 2. PCL, PCL-CTS and PCL-CTS-ECM electrospun scaffolds showed characteristic endothermic (melting) transformation points at 65 ºC, 64 ºC and 64 ºC, respectively (Figure 4A) [14, 15, 21]. The melting temperatures (T_m) were similar to the one from the PCL polymer (Table 2). CTS exhibited a melting temperature of 84.54 ºC. The PCL electrospun scaffold had a degradation temperature (T_d) of 391 ºC, which was lower than the value obtained for PCL polymer (410 ºC), as reported in the literature [14]. PCL-CTS and PCL-CTS-ECM scaffolds had degradation temperatures of 406 ºC and 408 ºC, respectively, which were higher than the PCL scaffold (Figure 4B). CTS showed two degradation steps: a slight degradation at the beginning of the analysis, as can be easily observed in Figure 4C and 4D, and a clear degradation at 298 ºC. The presence of dECM has no significant effect on the thermal properties of the scaffolds, which is in accordance with previous studies from our group [17].

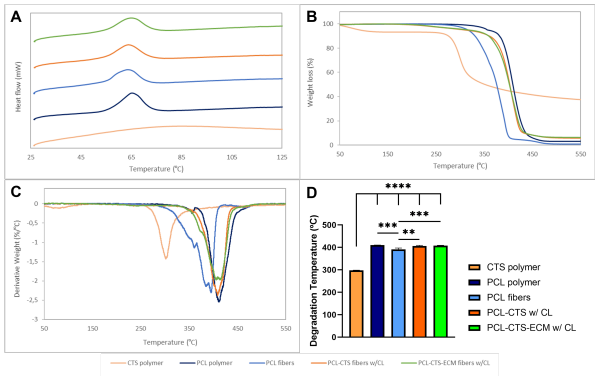

Figure 4: DSC (A), TGA (B) and DTGA (C) plots of PCL and CTS polymers, PCL, PCL-CTS and PCL-CTS-ECM electrospun scaffolds. D) Statistical analysis of degration temperature (T_d). For each condition, three different samples (N=3) were used in the analysis; ** $p < 0.01$, *** $p < 0.001$, **** $p < 0.0001$.

Table 2: Thermal properties of PCL and CTS polymers, PCL, PCL-CTS and PCL-CTS-ECM electrospun scaffolds

	PCL polymer	CTS polymer	PCL fibers	PCL-CTS fibers	PCL-CTS-ECM fibers
T_m (ºC)	65.42 $\pm$ 0.50	84.54 $\pm$ 1.31	64.84 $\pm$ 1.13	64.29 $\pm$ 0.29	64.44 $\pm$ 0.50
Weight loss (%)	96.70 $\pm$ 0.65	61.53 $\pm$ 0.77	99.83 $\pm$ 0.24	95.92 $\pm$ 2.89	93.69 $\pm$ 0.45
T_d (ºC)	410.27 $\pm$ 0.33	298.30 $\pm$ 0.22	390.88 $\pm$ 5.20	406.48 $\pm$ 2.52	408.10 $\pm$ 0.93

3.3.4. Contact Angle

PCL scaffolds were hydrophobic, since they presented an average contact angle of 109 ± 4°, a value comparable to those obtained by other authors [14, 18, 21]. PCL-CTS and PCL-CTS-ECM scaffolds were hydrophilic, since they showed average contact angle values of 47 ± 2°and 44 ± 3°, respectively [18, 21]. The addition of CTS to the scaffolds resulted in a significant decrease of the contact angle in comparison to the PCL scaffold.

3.3.5. Mechanical Tensile Testing

Results of mechanical tensile testing (Table 3) showed that PCL-CTS and PCL-CTS-ECM scaffolds exhibited decreased elastic modulus, UTS and elongation compared to PCL scaffolds, in agreement with the literature [15, 16, 18]. The addition of CTS in the electrospun scaffolds led to a decrease of the mechanical properties due its brittle behaviour. The incorporation of ECM did not greatly affect the mechanical properties of the PCL-CTS electrospun scaffolds [17].

Table 3: Mechanical properties of PCL, PCL-CTS and PCL-CTS-ECM electrospun scaffolds. Values as mean ± SD.

Scaffold	Modulus (MPa)	UTS (MPa)	Elongation (%)
PCL	1.276 ± 0.114	0.3172 ± 0.030	41.34 ± 4.78
PCL-CTS	1.057 ± 0.085	0.103 ± 0.031	20.27 ± 3.24
PCL-CTS-ECM	0.956 ± 0.038	0.108 ± 0.036	19.72 ± 3.32

3.4. Biological Effects of Electrospun Scaffolds

3.4.1. PDLSC Proliferation Assay and Cell Morphology Assessment

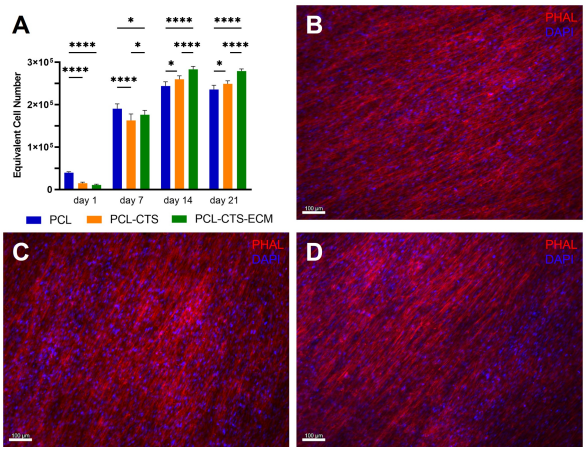

Figure 5: PDLSC proliferation assay (A) on PCL, PCL-CTS and PCL-CTS-ECM electrospun scaffolds. For each condition, six different samples (N=6) were used in the analysis; * $p < 0.05$, **** $p < 0.0001$. Cell morphology assessment by DAPI-Phalloidin staining on PCL (B), PCL-CTS (C) and PCL-CTS-ECM (D) electrospun scaffolds. Scale bar 100 µm.

The average number of viable PDLSCs per scaffold on days 1, 7, 14 and 21 is represented in Figure 5A. On days 1 and 7, PCL scaffolds showed higher numbers of cells compared to PCL-CTS and PCL-CTS-ECM scaffolds. However, it is important to note that PCL-CTS-ECM scaffolds showed a larger growth in the number of cells between days 1 and 7. On days 14 and 21, PCL-CTS and PCL-CTS-ECM scaffolds showed higher number of cells than PCL scaffolds. PCL-CTS scaffolds have been reported to show increased cell viability compared to PCL scaffolds [14, 21, 22]. On days 7, 14 and 21 days, there was a statistically significant increase in cell number on PCL-CTS-ECM scaffolds compared to PCL-CTS scaffolds, which suggests enhanced cell proliferation due to the presence of dECM in the scaffold as seen in the literature [17].

After 21 days of osteogenic differentiation, PDLSCs seeded on all electrospun scaffolds presented similar morphology (Figure 5). PDLSCs were very densely organized and seemed similarly distributed across on all electrospun scaffolds.

3.4.2. Immunocytochemistry Analysis

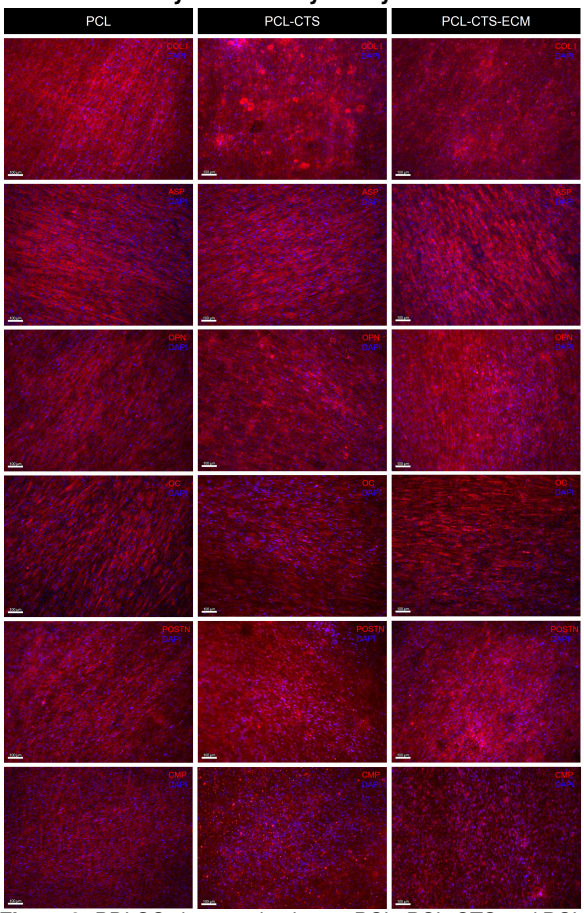

Figure 6: PDLSC characterization on PCL, PCL-CTS and PCL-CTS-ECM scaffolds by immunocytochemistry analysis. Immunofluorescent staining images of collagen I (COL I, red), asporin (ASP, red), osteopontin (OPN, red), osteocalcin (OC, red), periostin (POSTN, red) and cementum protein (CMP, red). Nuclei were counterstained with DAPI (blue). Scale bar 100 µm.

The expression of various proteins by PDLSCs on PCL, PCL-CTS and PCL-CTS-ECM electrospun scaffolds after 21 days of osteogenic differentiation is illustrated in Figure 6. Overall, PDLSCs seeded on all scaffolds showed a positive expression of collagen I, asporin, osteopontin, osteocalcin, periostin and cementum protein. PDLSCs showed a

more visible expression of POSTN than CMP, suggesting an enhanced PDLSCs commitment to osteoblasts instead of cementoblasts, as a direct result from the osteogenic differentiation performed. No significant differences with regards to the immunofluorescent staining images were observed between the different types of scaffolds. Incorporation of chitosan in PCL nanofibers has been reported to increase the expression of osteopontin in murine pre-osteoblast cells [23].

3.4.3. ALP Activity Assay

After 21 days of osteogenic differentiation, PDLSCs cultured on PCL-CTS-ECM scaffolds presented higher ALP activity values compared to PCL and PCL-CTS scaffolds, as can be observed in Figure 7. An increase in ALP activity has been reported in the literature in scaffolds with ECM incorporated [9, 17]. Furthermore, there was also an increase in ALP activity in PCL-CTS scaffolds compared to PCL scaffolds, which has been also reported in the literature [22, 23].

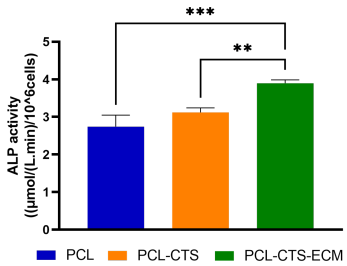

Figure 7: ALP activity normalized to the number of cells present on PCL, PCL-CTS and PCL-CTS-ECM electrospun scaffolds. Values are expressed as mean ± SD. For each experimental group, three different samples (N=3) were used in the analysis; ** $p < 0.01$, *** $p < 0.001$.

3.4.4. Biomineralization Staining

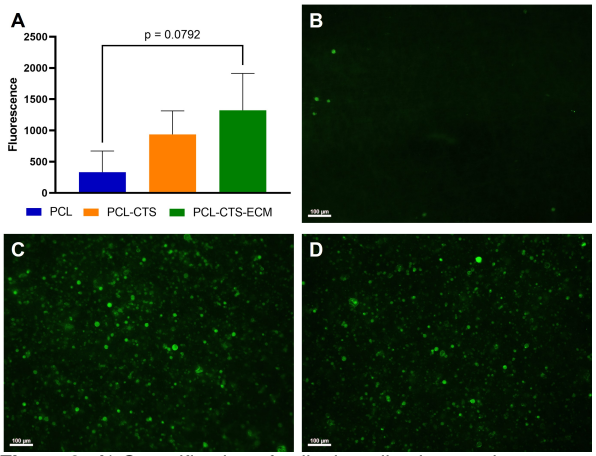

Figure 8: A) Quantification of cell mineralization on electrospun scaffolds. Values are expressed as mean ± SD. Three different samples (N=3) were used in the analysis. Fluorescent staining of cell mineralization on PCL (B), PCL-CTS (C) and PCL-CTS-ECM (D) electrospun scaffolds. Scale bar 100 µm.

Fluorescent staining images confirm cell mineralization on PCL-CTS and PCL-CTS-ECM scaffolds, showing more intense fluorescence in comparison to PCL scaffolds, as can be observed in Figure 8B-D. The quantification of the fluorescent staining confirmed higher levels of cell mineralization on PCL-CTS and PCL-CTS-ECM scaffolds in comparison to PCL scaffolds. There was an increase in fluorescence in PCL-CTS-ECM scaffolds in comparison to PCL-CTS scaffolds. (Figure 8A)

3.4.5. Alizarin Red Staining and Quantification

Alizarin Red staining confirmed calcium deposition (in red) on PCL, PCL-CTS and PCL-CTS-ECM electrospun scaffolds (Figures 9B-D). On PCL-CTS and PCL-CTS-ECM scaffolds large calcium deposits were clearly visible, which were not present on PCL scaffolds. Alizarin Red quantification (Figure 9A) confirmed a significant increase in calcium deposition on PCL-CTS and PCL-CTS-ECM in comparison to PCL scaffolds, which lays in agreement with previous studies [22, 23].

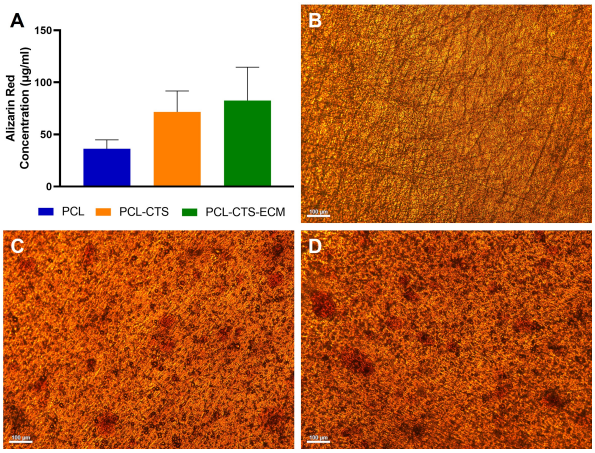

Figure 9: A) Quantification of Alizarin Red staining bound to PCL, PCL-CTS and PCL-CTS-ECM scaffolds. Values are expressed as mean ± SD. Three different samples (N=3) were used in the analysis. Alizarin staining of PDLSCs on PCL (B), PCL-CTS (C) and PCL-CTS-ECM (D) scaffolds.

3.4.6. Gene expression analysis

Gene expression analysis (Figure 10) confirmed the results from the ALP activity assay. ALP expression was downregulated in PCL, sustained in PCL-CTS and significantly upregulated in PCL-CTS-ECM scaffolds. All scaffolds showed upregulated expression of Runx2 and OSX, which are key genes involved in osteogenic differentiation. Although PCL scaffolds showed increased upregulation of Runx2 and OSX expression, the associated standard error was elevated. All scaffolds showed similar downregulated expression of CMP and upregulated OC expression. A decreased expression of CMP, was also seen in the immunofluorescent staining, which supports the commitment of PDLSCs to osteoblasts instead of cementoblasts. Col I expression was significantly upregulated in PCL-CTS and even more in PCL-CTS-

ECM scaffolds, whilst in PCL scaffolds it was maintained. Overall, the use of PDLSC-derived ECM has been shown to enhance osteogenic differentiation by increased calcium deposition, ALP activity and osteogenic marker expression, as previously reported in the literature [9, 24].

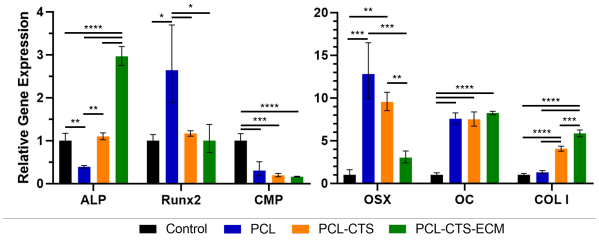

Figure 10: Effects of electrospun scaffolds on ALP, RUNX2, CMP1, OSX, OC and Col I gene expression by PDLSCs after 21 days of osteogenic differentiation. Results presented as fold change expression relative to undifferentiated PDLSCs at day 0 (Control). Values are expressed as mean ± SD (N=3). * $p < 0.05$, ** $p < 0.01$, *** $p < 0.001$, **** $p < 0.0001$.

4. Conclusions

This work's findings reveal maintained expression of proteins present in PDLSCs after decellularization process. Decellularized cell-derived ECM showed a fibrillary structure and retained GAG and collagen content present before decellularization process. Successful decellularization was confirmed with residual DAPI staining in dECM and diminished DNA content. Results demonstrate that PCL-CTS-ECM scaffolds maintained similar physical and mechanical properties of PCL-CTS scaffolds. The incorporation of dECM did not greatly alter the scaffolds' characteristics. PCL-CTS and PCL-CTS-ECM scaffolds presented differences in comparison to PCL scaffolds, with regards to structure, thermal degradation, hydrophilicity and mechanical properties. PCL-CTS-ECM scaffolds significantly promoted cell proliferation compared to PCL and PCL-CTS scaffolds, which results from the presence of dECM. PDLSCs populated densely and showed a positive expression of Col I, ASP, OPN, OC and POSTN on all scaffolds. The upregulated expression of Runx2, OSX and OC, in addition to the visualized positive expression of OPN, OC and POSTN, confirm successful osteogenic differentiation of PDLSCs on all scaffolds. PCL-CTS-ECM scaffolds enhanced osteogenic differentiation of PDLSCs, which was confirmed by increased levels of ALP activity and calcium deposition. PCL-CTS scaffolds showed higher levels of calcium deposition and cell mineralization than PCL scaffolds. All in all, results show that cell-derived ECM electrospun scaffolds enhanced the proliferation and osteogenic differentiation of PDLSCs. This work describes the first use of lyophilized cell-derived ECM loaded electrospun scaffolds for periodontal tissue engineering applications and and highlights its potential for the treatment of periodontitis. Future studies on the ECM loaded electrospun scaffolds still need to be conducted to assess their antibacterial properties and optimize dECM amounts for improved periodontal tissue differentiation and maturation.

5. Acknowledgments

This document was written and made publically available as an institutional academic requirement and as a part of the evaluation of the MSc thesis in Biomedical Engineering of the author at Instituto Superior Técnico (IST). The work described herein was performed at the Institute for Bioengineering and Biosciences of IST (Lisbon, Portugal), during the period March-October 2022, under the supervision of Dr. João Carlos Fernandes da Silva and Dr. Marta Monteiro Silva Carvalho.

References

[1] Preshaw et al. Current concepts in periodontal pathogenesis. *Dental Update*, 31(10):570–578, 2004.
[2] Zhao et al. Electrospun nanofibers for periodontal treatment: A recent progress. *International Journal of Nanomedicine*, 17:4137–4162, 2022.
[3] Zhuang et al. Advance of nano-composite electrospun fibers in periodontal regeneration. *Frontiers in Chemistry*, 7, 7 2019.
[4] Guarino et al. Electrospun polycaprolactone nanofibres decorated by drug loaded chitosan nano-reservoirs for antibacterial treatments. *Nanotechnology*, 28, 11 2017.
[5] Khodir et al. Trapping tetracycline-loaded nanoparticles into polycaprolactone fiber networks for periodontal regeneration therapy. *Journal of Bioactive and Compatible Polymers*, 28:258–273, 5 2013.
[6] Shalumon et al. Effect of incorporation of nanoscale bioactive glass and hydroxyapatite in pcl/chitosan nanofibers for bone and periodontal tissue engineering. *Journal of Biomedical Nanotechnology*, 9:430–440, 3 2013.
[7] Sundaram et al. Bilayered construct for simultaneous regeneration of alveolar bone and periodontal ligament. *Journal of Biomedical Materials Research - Part B Applied Biomaterials*, 104:761–770, 5 2016.
[8] Seo et al. Investigation of multipotent postnatal stem cells from human periodontal ligament. *Lancet*, 364:149–155, 7 2004.
[9] Heng et al. Effects of decellularized matrices derived from periodontal ligament stem cells and shed on the adhesion, proliferation and osteogenic differentiation of human dental pulp stem cells in vitro. *Tissue and Cell*, 48(2):133–143, 2016.
[10] Xing et al. Extracellular matrix-derived biomaterials in engineering cell function. *Biotechnology Advances*, 42:107421, 2020.
[11] Silva et al. Compositional and structural analysis of glycosaminoglycans in cell-derived extracellular matrices. *Glycoconjugate Journal*, 36:141–154, 4 2019.
[12] Carvalho et al. Cultured cell-derived extracellular matrices to enhance the osteogenic differentiation and angiogenic properties of human mesenchymal stem/stromal cells. *Journal of Tissue Engineering and Regenerative Medicine*, 13:1544–1558, 9 2019.
[13] Gao et al. Strategy of a cell-derived extracellular matrix for the construction of an osteochondral interlayer. *Biomaterials Science*, 2022.
[14] Lorenzo et al. Electrospun polycaprolactone/chitosan scaffolds for nerve tissue engineering: Physicochemical characterization and schwann cell biocompatibility. *Biomedical Materials*, 12, 2 2017.
[15] Zou et al. Electrospun chitosan/polycaprolactone nanofibers containing chlorogenic acid-loaded halloysite nanotube for active food packaging. *Carbohydrate Polymers*, 247, 11 2020.
[16] Hadjianfar et al. Polycaprolactone/chitosan blend nanofibers loaded by 5-fluorouracil: An approach to anticancer drug delivery system. *Polymers for Advanced Technologies*, 29:2972–2981, 12 2018.
[17] Carvalho et al. Co-culture cell-derived extracellular matrix loaded electrospun microfibrous scaffolds for bone tissue engineering. *Materials Science and Engineering C*, 99:479–490, 6 2019.
[18] Zhu et al. Electrospun metformin-loaded polycaprolactone/chitosan nanofibrous membranes as promoting guided bone regeneration membranes: Preparation and characterization of fibers, drug release, and osteogenic activity in vitro. *Journal of Biomaterials Applications*, 34:1282–1293, 4 2020.
[19] Ye et al. Enhanced osteogenesis and angiogenesis by pcl/chitosan/sr-doped calcium phosphate electrospun nanocomposite membrane for guided bone regeneration. *Journal of Biomaterials Science, Polymer Edition*, 30:1505–1522, 11 2019.
[20] Liverani et al. Incorporation of bioactive glass nanoparticles in electrospun pcl/chitosan fibers by using benign solvents. *Bioactive Materials*, 3:55–63, 3 2018.
[21] Urbanek et al. Structure and properties of polycaprolactone/chitosan nonwovens tailored by solvent systems. *Biomedical Materials*, 12, 2 2017.
[22] He et al. Osteogenic induction of bone marrow mesenchymal cells on electrospun polycaprolactone/chitosan nanofibrous membrane. *Dental Materials Journal*, 36:325–332, 2017.
[23] Yang et al. Acceleration of osteogenic differentiation of preosteoblastic cells by chitosan containing nanofibrous scaffolds. *Biomacromolecules*, 10:2772–2778, 10 2009.
[24] Farag et al. The effect of decellularized tissue engineered constructs on periodontal regeneration. *Journal of Clinical Periodontology*, 45:586–596, 5 2018.